



OREGON STATE UNIVERSITY

2019 NASA SL TEAM

104 KERR ADMIN BLDG. # 1011

CORVALLIS, OR 97331

---

## Post-Launch Assessment Review

---

April 29th, 2019

## CONTENTS

<b>1</b>	<b>Summary of PLAR Report</b>	6
1.1	Team Summary . . . . .	6
1.2	Launch Vehicle Summary . . . . .	6
1.3	Payload Summary . . . . .	6
<b>2</b>	<b>Mission Summary</b>	7
2.1	Mission Overview . . . . .	7
<b>3</b>	<b>Launch Vehicle Summary</b>	8
3.1	Launch Vehicle Overview . . . . .	8
3.2	Motor Choice . . . . .	9
3.3	Mission Performance Predictions . . . . .	9
3.3.1	Altitude Predictions . . . . .	9
3.3.2	Landing Kinetic Energy Predictions . . . . .	10
3.3.3	Descent Time Predictions . . . . .	10
3.3.4	Drift Predictions . . . . .	11
3.4	Data Analysis . . . . .	12
3.4.1	Altimeter Data . . . . .	12
3.4.2	Drift Data . . . . .	15
3.4.3	Coefficient of Drag . . . . .	16
3.5	Flight Anomalies . . . . .	17
3.5.1	Recovery Anomaly . . . . .	18
3.5.2	Camera System Anomaly . . . . .	19
3.5.3	Damage Summary . . . . .	20
3.6	Differences Between Predicted and Actual Data . . . . .	22
<b>4</b>	<b>Payload Summary</b>	24
4.1	Payload Overview . . . . .	24
4.2	Data Analysis and Results . . . . .	24
4.3	Payload Anomalies . . . . .	24
4.4	Visual Observations . . . . .	26
4.5	Scientific Value . . . . .	27
<b>5</b>	<b>Project Plan</b>	30
5.1	Budget Summary . . . . .	30
5.2	STEM Engagement Summary . . . . .	30

<b>6</b>	<b>Lessons Learned</b>	<b>31</b>
<b>7</b>	<b>Experience Summary</b>	<b>31</b>

**LIST OF TABLES**

1	Team Summary Chart	6
2	Landing Kinetic Energy	10
3	Landing Kinetic Energy of Full Scale Launch	10
4	Drift and Descent Time	11
5	Ascent Data	13
6	Descent and Impact Data	15
7	Major funding contributions breakdown.	30

## LIST OF FIGURES

1	A depiction of the mission profile (NTS) . . . . .	7
2	Final Launch Vehicle CAD . . . . .	8
3	Final Launch Vehicle Components CAD . . . . .	8
4	Motor Thrust Curve of Cesaroni L2375-WT . . . . .	9
5	OpenRocket Model . . . . .	9
6	Descent Trajectory . . . . .	11
7	Competition Flight Plot . . . . .	12
8	Ascent Data . . . . .	13
9	Fore Descent Data . . . . .	14
10	Aft Descent Data . . . . .	15
11	Fore section drift . . . . .	16
12	Aft section drift . . . . .	16
13	Drag coefficient based on altimeter data . . . . .	17
14	Aft airframe during recovery . . . . .	18
15	Tangled shroud lines . . . . .	19
16	Canister Damage . . . . .	20
17	BEAVS Damage . . . . .	21
18	Airframe Damage . . . . .	21
19	Aft Ejection Bay Damage . . . . .	22
20	2017-2018 Field Conditions . . . . .	25
21	2018-2019 Field Conditions . . . . .	25
22	Rover Landing Spot . . . . .	26
23	Distance from the fore airframe . . . . .	27
24	Fore measurement . . . . .	27
25	Distance from the nosecone . . . . .	27
26	Nosecone measurement . . . . .	27
27	Distance from the shock cord . . . . .	27
28	Shock cord measurement . . . . .	27
29	Scientific Base Station . . . . .	28

## ACRONYM DICTIONARY

**9DOF** Nine Degrees of Freedom. [6](#)

**AGL** Above Ground Level. [6, 12–14](#)

**AIAA** American Institute of Aeronautics and Astronautics. [30](#)

**ASL** Above Sea Level. [9](#)

**ATI** Allegheny Technologies Incorporated. [30](#)

**ATU** Avionics Telemetry Unit. [15, 22](#)

**BEAVS** Blade Extending Apogee Variance System. [4, 8, 20, 21](#)

**CAD** Computer-Aided Design. [4, 8](#)

**FHP** Fore Hard Point. [8](#)

**FRR** Flight Readiness Review. [22, 24](#)

**GPS** Global Positioning System. [6, 7, 15, 24, 25, 28](#)

**ICE** Innovative Composite Engineering. [8, 30](#)

**IMU** Inertial Measurement Unit. [6](#)

**MPRL** Machine Product and Realization Laboratory. [22](#)

**NASA** National Aeronautics and Space Administration. [28, 30](#)

**NTS** Not To Scale. [4, 7](#)

**OSGC** Oregon Space Grant Consortium. [30](#)

**OSRT** Oregon State Rocketry Team. [6, 7, 10, 17, 19, 20, 22, 24, 26–31](#)

**OSU** Oregon State University. [22, 30, 31](#)

**PEARS** Payload Ejection and Retention System. [8, 24](#)

**PLA** Polylactic Acid. [22](#)

**PLEC** Payload Ejection Controller. [24](#)

**RDO** Rover Deployment Officer. [7](#)

**RSO** Range Safety Officer. [19](#)

**SCAR** Soil Collection and Retention. [24](#)

**SL** Student Launch. [10, 30](#)

**SLI** Student Launch Initiative. [31](#)

**STEM** Science, Technology, Engineering and Mathematics. [30, 31](#)

## 1 SUMMARY OF PLAR REPORT

### 1.1 Team Summary

Table 1: Team Summary Chart

Team Name	Oregon State Rocketry Team
Mailing Address	104 Kerr Admin Bldg #1011 Corvallis, OR 97331
Name of Mentor	Joe Bevier
NAR/TRA Number, Certification Level	NAR #87559 Level 3, TRA #12578 Level 3
Contact Information	joebevier@gmail.com, (503) 475-1589

### 1.2 Launch Vehicle Summary

The launch vehicle was 129 in. long and weighed 57.7 lbf, including ballast. The selected motor was a Cesaroni Cesaroni L2375-WT. The launch vehicle targeted an apogee altitude of 4,500 ft and launched from a 1515, 12 ft rail with a simulated rail exit velocity of 83.4 ft/s. The airframe was a 6.25 in. inner diameter fiberglass and carbon fiber tube. The launch vehicle was recovered in two independent sections: the aft section with the motor, and the fore section with the payload and nosecone. At apogee, the launch vehicle had two simultaneous separation events: the aft section separated from the fore section and released the first drogue parachute, and the fore section separated from the nosecone and released the second drogue parachute. The main parachutes were retained with two Tender Descenders in series and released at 800 ft [Above Ground Level \(AGL\)](#). 1.0 and 1.5 seconds after the Tender Descenders ignited, primary and secondary ejection charges were ignited, ensuring the main parachute left the airframe. The drogue parachutes were 1.5 ft in diameter and cruciform in shape. The main parachutes were toroidal in shape and 8 ft in diameter.

### 1.3 Payload Summary

The [Oregon State Rocketry Team \(OSRT\)](#) built a deployable rover that collects a soil sample. The rover was contained within the fore section of the airframe. Upon landing, the rover was ejected from the airframe using black powder charges. It had two coaxial, independently driven wheels with a chassis suspended between them. A spring-loaded stabilizer arm acted as a third point of contact with the ground. An Arduino Teensy 3.6 microcontroller autonomously controlled the motors to move the rover, receiving input from a sensor array including sonar, [Global Positioning System \(GPS\)](#), and a [Nine Degrees of Freedom \(9DOF\) Inertial Measurement Unit \(IMU\)](#). An auger was mounted at the midpoint of the chassis. When the rover is deployed the auger periodically gathers soil samples and seals them in an internal containment unit. After collection, the rover was to autonomously drive to a scientific base station where it would perform an additional scientific experiment.

## 2 MISSION SUMMARY

### 2.1 Mission Overview

The planned mission for [OSRT](#) was to launch off of a 12 ft 1515 launch rail with a Cesaroni L2375-WT. After motor burnout, the launch vehicle coasted to a targeted apogee of 4,500 ft, separating into two independent sections. Two drogue parachutes were deployed, followed by two main parachutes at an altitude of 800 ft. After landing under kinetic energy, descent time, and drift radius requirements, and upon clearance from the [Rover Deployment Officer \(RDO\)](#), the payload was to remotely deploy from the aft end of the fore section of the airframe. The payload then would autonomously navigate away from the airframe before collecting and sealing a soil sample. After validation of the soil sample being collected, the rover would deposit a soil sample at a scientific base station for a pH measurement. The pH and [GPS](#) coordinates of the soil sample were to be sent back to the ground station, and the rover repeated the process for additional samples until battery failure. This would allow [OSRT](#) to generate a pH map of the landing site. Shown in Figure 1 is a graphic representation of the mission profile.

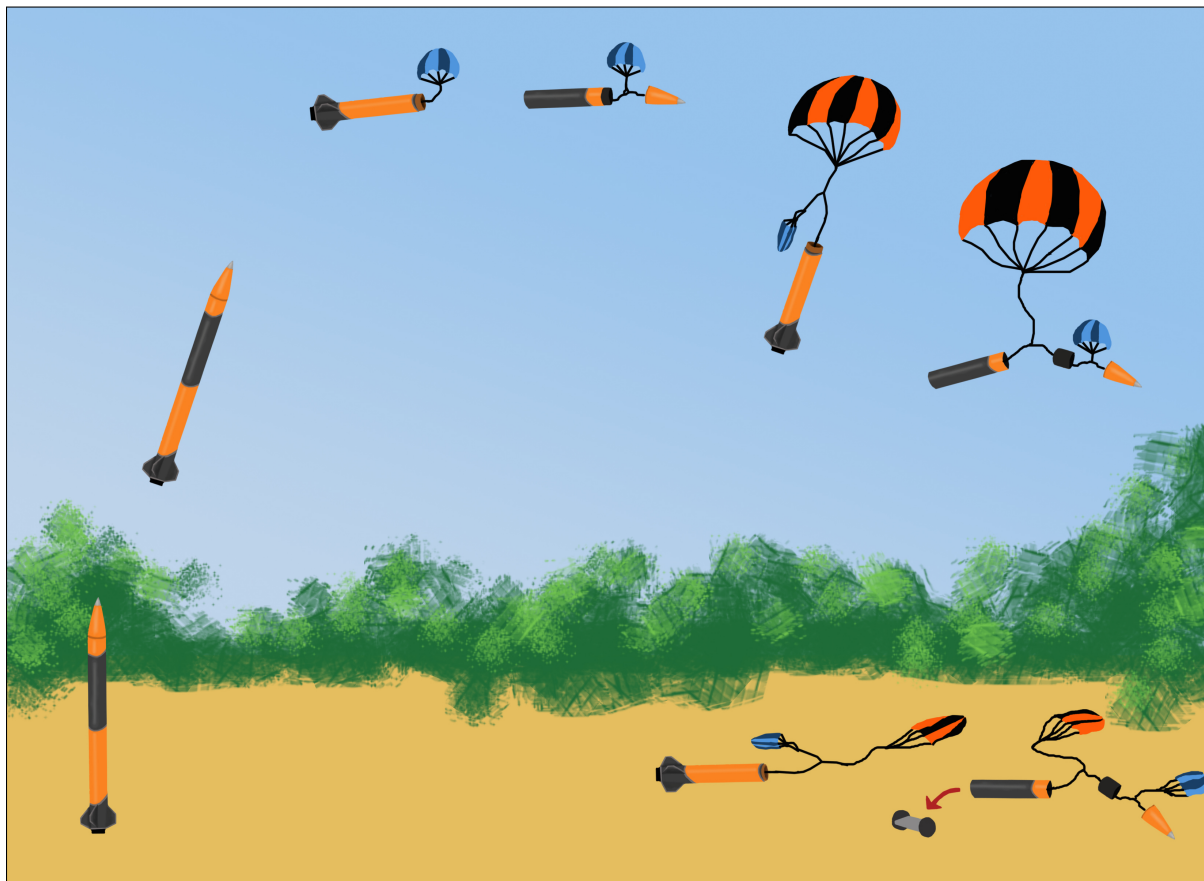


Figure 1: A depiction of the mission profile ([Not To Scale \(NTS\)](#)).

### 3 LAUNCH VEHICLE SUMMARY

#### 3.1 Launch Vehicle Overview

The launch vehicle was 129 in. in length with a 6.25 in. inner diameter airframe. The nosecone was a 5:1 ogive nosecone with an aluminum tip, cut to match the outer diameter of the airframe. The fore section of the airframe was fiberglass, while the aft section was carbon fiber in the motor tube section and seamlessly transitioned to fiberglass above the motor tube. Both airframes were made to a 6.25 in. inner diameter and manufactured at [Innovative Composite Engineering \(ICE\)](#). The nosecone coupler was laid up of 18 plies of fiberglass, co-bonded directly to the inside of the nosecone. The aft coupler was laid up of 18 plies of fiberglass. Three centering rings were epoxied into the airframe to permanently attach the motor tube. Four trapezoidal fins made of 1/8 in. carbon fiber plate were permanently attached to the airframe using G5000 RocketPoxy fillets on the motor tube, inside of the airframe, and outside of the airframe. The [Computer-Aided Design \(CAD\)](#) model of the exterior of the airframe is depicted in Figure 2.

The components within the nosecone were the fore avionics bay and the nosecone pressure seal, designed to reduce ejection charge sizes. The components within the fore airframe from fore to aft were: fore main and drogue parachutes, fore pressure seal and radial bolt ring, fore ejection bay, fore ballast bay, [Fore Hard Point \(FHP\)](#), [Payload Ejection and Retention System \(PEARS\)](#), and the rover. The components within the aft section from fore to aft were: aft main and drogue parachutes, aft pressure seal and radial bolt ring, aft ejection bay, aft avionics bay, 360° camera system, aft ballast bay, the [Blade Extending Apogee Variance System \(BEAVS\)](#), and the motor and fins. The [CAD](#) models of the components are shown in Figure 3, parachutes are not shown.



Figure 2: Final Launch Vehicle [CAD](#)

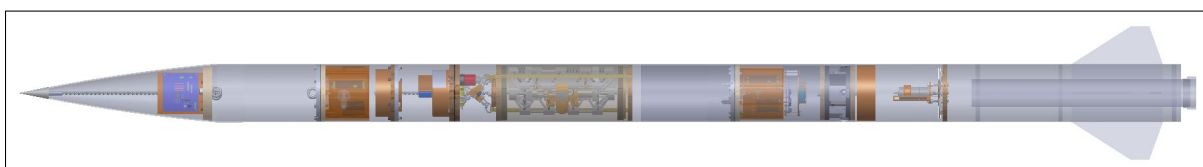


Figure 3: Final Launch Vehicle Components [CAD](#)

### 3.2 Motor Choice

A Cesaroni L2375-WT motor was used for flight at competition. The average thrust of the selected motor is 534 lbf with a burn time of 2.07 s. The motor thrust curve of the Cesaroni L2375-WT motor can be seen in Figure 4. The total weight of the launch vehicle on the launch rail was 57.7 lbf. The launch vehicle therefore had a thrust to weight ratio of 9.25.

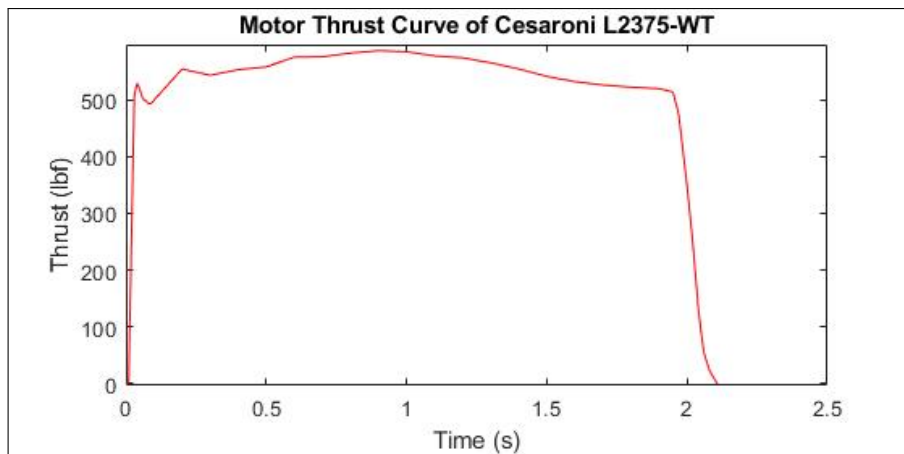


Figure 4: Motor Thrust Curve of Cesaroni L2375-WT

### 3.3 Mission Performance Predictions

#### 3.3.1 Altitude Predictions

OpenRocket was used to predict the apogee altitude of the launch vehicle at Bragg Farms in Huntsville, AL. Input into the simulation were varying wind speeds, a launch pad altitude [Above Sea Level \(ASL\)](#) of 600 ft, and a launch rail angle of 5°. For the launch day, ballast configuration for 0 mph winds was chosen. A 0.5 lbf ballast bay was used in the aft section. The stability margin of the launch vehicle with the aft ballast bay remained above the required 2.0 calibers with a stability margin of 2.12 calibers. The predicted apogee altitude of the launch vehicle on launch day was predicted to be 4,507 ft. The OpenRocket model can be seen in Figure 5.

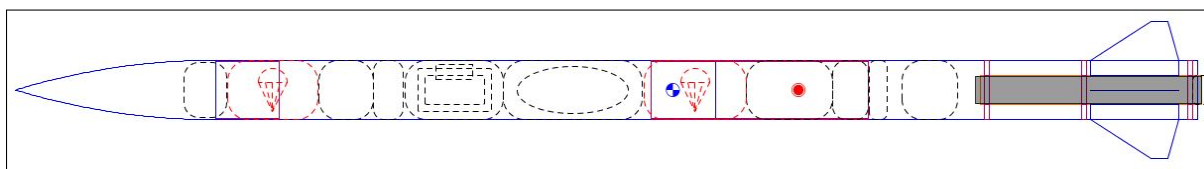


Figure 5: OpenRocket Model

### 3.3.2 Landing Kinetic Energy Predictions

A MATLAB script was used to calculate the landing kinetic energies of each recovered section of the airframe. This code was verified to be accurate based on the results of the subscale and the full scale launches. On average, the subscale and full scale launch vehicle has descended slightly slower than what the simulations predict. This provides the OSRT with a small safety factor. The weight, landing velocity, and landing kinetic energy of each section are shown in Table 2. It can be seen that with both main parachutes successfully deploying, the kinetic energy at landing is under the maximum value of 75 ft-lbf.

Table 2: Landing Kinetic Energy

Measurement	Fore Section	Aft Section	Nosecone
Weight [lbf]	18.2	20.1	5.1
Velocity with Main and Drogue Deployed [ft/s]	15.1	14.2	15.1
Kinetic Energy with Main and Drogue Deployed [ft-lbf]	64.1	62.7	17.9
Velocity with Only Drogue Deployed [ft/s]	111.0	112.0	111.0
Kinetic Energy with Only Drogue Deployed [ft-lbf]	3,485.0	3,922.4	970.8
Velocity with No Parachutes Deployed [ft/s]	115.0	116.0	115.0
Kinetic Energy with No Parachutes Deployed [ft-lbf]	3,740.7	4,207.5	1,042.0

Based on simulations and altimeter data from OSRT's Vehicle Demonstration Flight, all recovery requirements in the Student Launch (SL) Handbook were met. The predicted kinetic energy at landing of these sections can be seen in Table 3.

Table 3: Landing Kinetic Energy of Full Scale Launch

Measurement	Fore Section	Aft Section	Nosecone
Weight (lbf)	18.201	20.121	5.070
Velocity with Main and Drogue Deployed [ft/s]	11.66	14.50	11.66
Kinetic Energy with Main and Drogue Deployed [ft-lbf]	38.455	65.92	10.71

### 3.3.3 Descent Time Predictions

A MATLAB script was written to predict the descent time of each section of the airframe. This simulation was verified to be accurate by the results of the first full scale launch. Under a 1.5 ft cruciform drogue parachute and a 8 ft toroidal main parachute for both the fore and the aft sections, the descent trajectories for both sections were calculated on MATLAB. This script accounts for the changing air densities at different altitudes and the acceleration of the launch vehicle at apogee and deployment. This is shown in Figure 6. It can be seen that both sections land in under 90 seconds. The exact predicted descent time can be seen in Table 4.

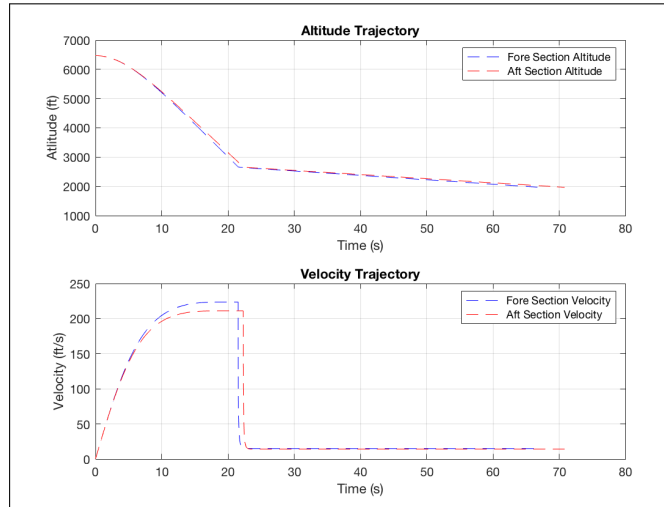


Figure 6: Descent Trajectory

### 3.3.4 Drift Predictions

A MATLAB script was written to predict the drift of the descending launch vehicle sections. This simulation was verified to be accurate by the results of the subscale and full scale launches. The wind speed was assumed to be a constant crosswind that does not impact the vertical trajectory. Weather cocking was not included in this calculation, so it was assumed that apogee occurred directly above the launch pad. This is a conservative approach because weather cocking pushes the launch vehicle the opposite direction of the drift. These calculations are shown in Table 4. These are compared with drift calculations from OpenRocket which does include weather cocking.

Table 4: Drift and Descent Time

Wind Speed (mph)	0	5	10	15	20	Descent Time (s)
Drift of the Fore Section (ft)	0	492	984	1,476	1,967	67.07
Drift of the Aft Section (ft)	0	519	1,039	1,558	2,077	70.830
OpenRocket Simulation (ft)	2	369	711	1,071	1,394	67.8

## 3.4 Data Analysis

### 3.4.1 Altimeter Data

The scoring altimeter at competition audibly read out a value of 4,548 ft **AGL**. After analyzing the logged data from the altimeters, apogee appeared to be slightly lower than what the altimeters output immediately following the launch. Figure 7 displays the flight path of the fore and aft sections of the launch vehicle.

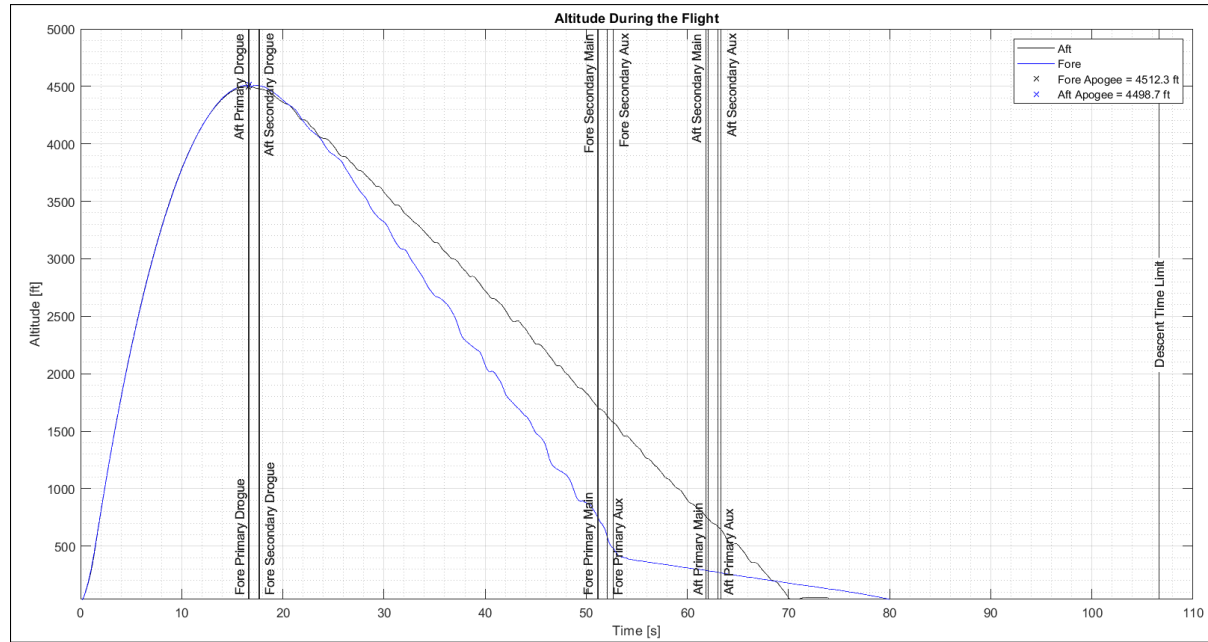


Figure 7: Competition Flight Plot

After taking the root mean squared for the fore section and the aft section altimeters, the data was plotted here. The aft section recorded an apogee of 4,498 ft **AGL** and the fore section recorded an apogee of 4,512 ft **AGL**.

Figure 8 shows the data collected during the ascent of the launch vehicle. Table 5 lists the apogee, maximum velocity, and acceleration during ascent. The apogee value is the root mean squared of all four altimeters.

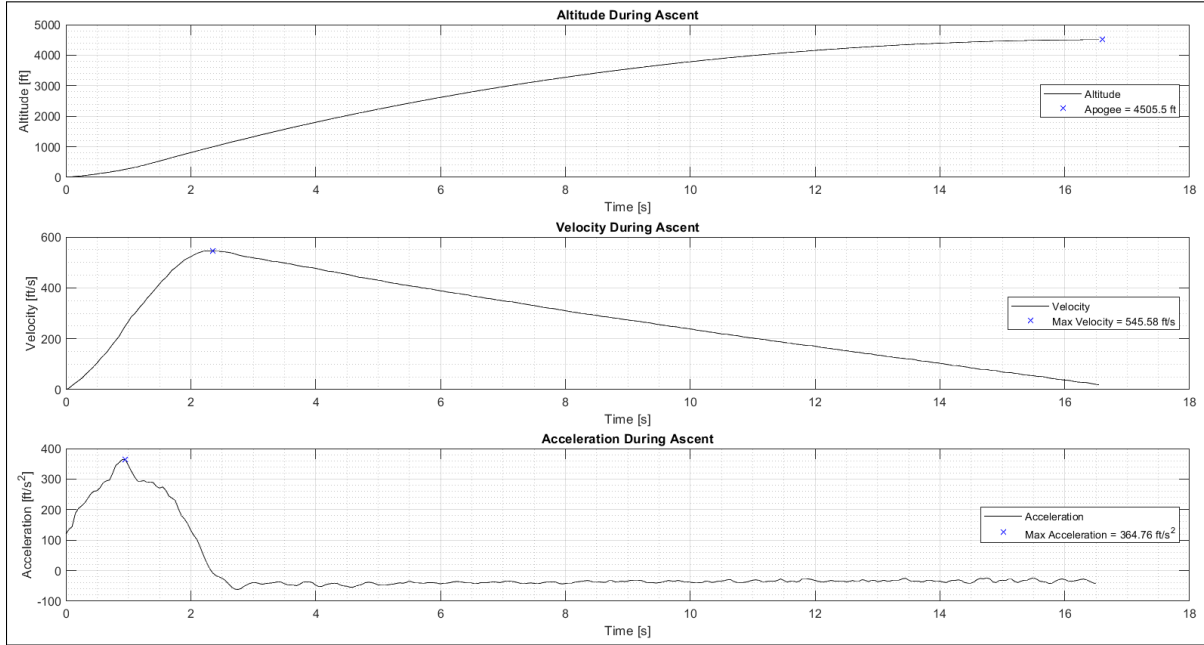


Figure 8: Ascent Data

Apogee [ft]	Maximum Velocity [ft/s]	Maximum Acceleration [ft/s <sup>2</sup> ]
4,505	546	365

Table 5: Ascent Data

Figure 9 shows the descent data recorded in the fore section of the launch vehicle. When the altimeters sensed 800 ft **AGL**, the Tender Descenders separated. This happened 51.15 and 51.20 seconds into the flight. The corresponding altitudes were 738.6 and 738.9 ft **AGL**. The auxiliary ports fired 52.10 and 52.70 seconds into the flight. The corresponding altitudes were 565.9 and 487.1 ft **AGL**. The main parachute inflated roughly 514 ft **AGL**.

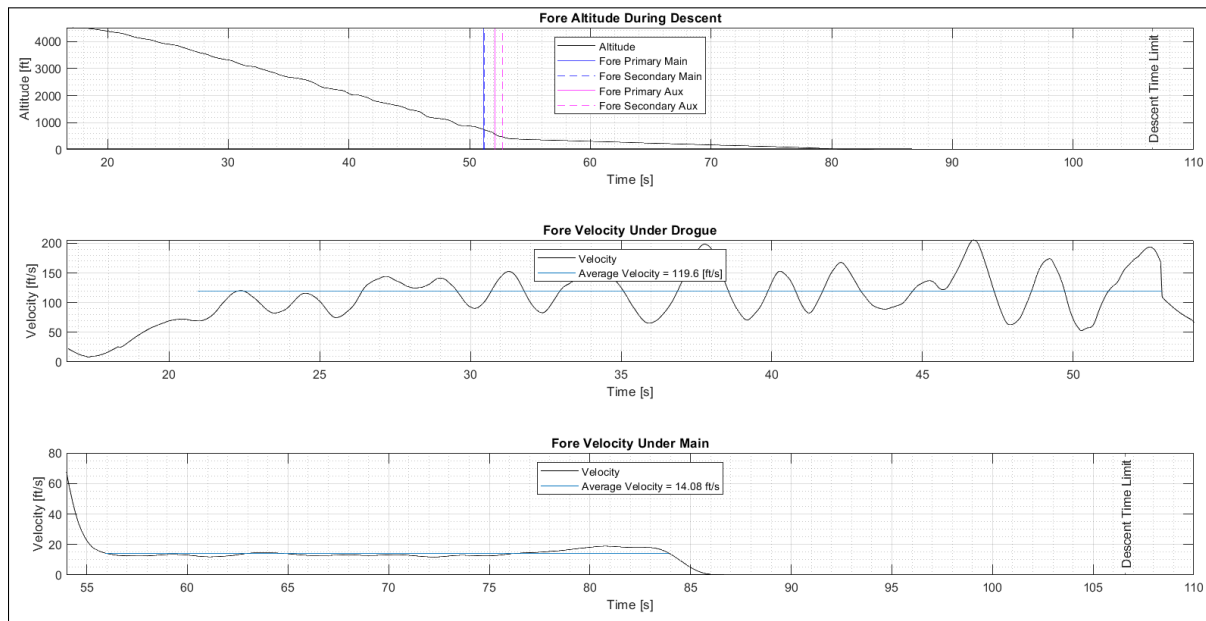


Figure 9: Fore Descent Data

Figure 10 shows the descent data recorded in the aft section of the launch vehicle. When the altimeters sensed 800 ft **AGL**, the Tender Descenders separated. This happened 62.05 and 61.85 seconds into the flight. The corresponding altitudes were 728.0 and 736.6 ft **AGL**. The auxiliary ports fired 63.05 and 63.35 seconds into the flight. The corresponding altitudes were 631.5 and 623.1 ft **AGL**. The main parachute on the aft section never opened due to the shroud lines becoming entangled with the rest of the riser.

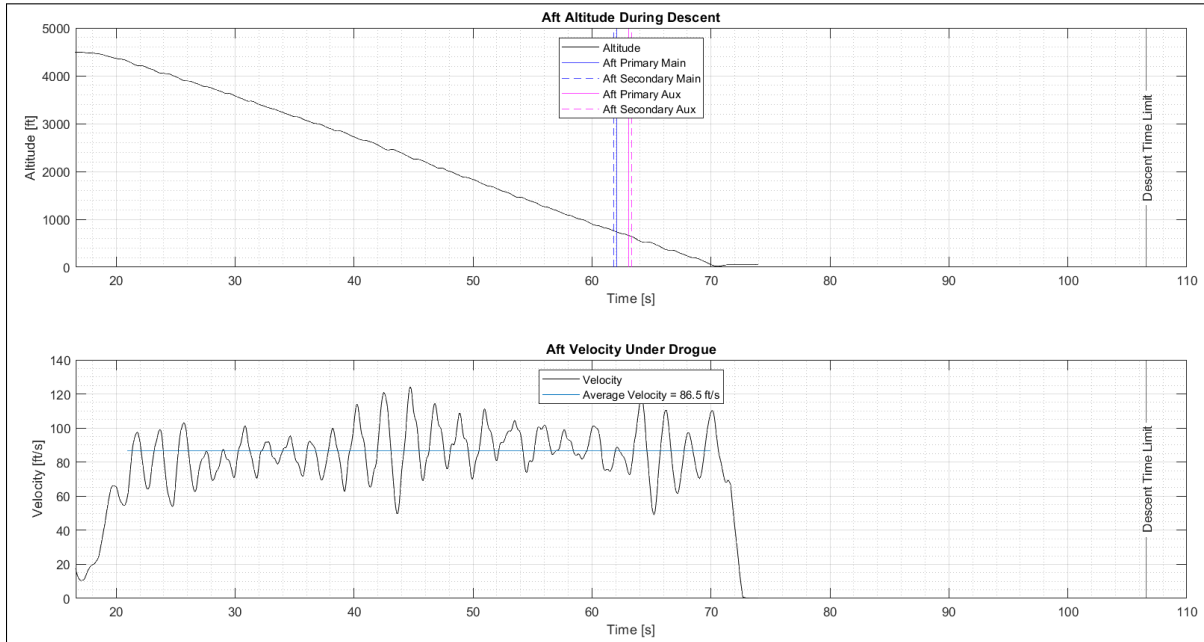


Figure 10: Aft Descent Data

Table 6 summarizes the weight, impact velocities, impact kinetic energies, and descent times of the launch vehicle sections.

Launch Vehicle Section	Weight [lb]	Impact Velocity [ft/s]	Impact Kinetic Energy [ft-lbf]	Descent Time [s]
Nosecone	5.32	15.71	20.38	65.40
Fore Airframe	17.43	15.71	66.76	65.40
Aft Airframe	21.28	65.21	1404.9	54.10

Table 6: Descent and Impact Data

### 3.4.2 Drift Data

The aft [Avionics Telemetry Unit \(ATU\)](#) reported a maximum in-flight drift distance of 2,275 ft and a final drift distance of 471 ft. The fore [ATU](#) reported a maximum in-flight drift distance of 1,876 ft and a final drift distance of 952 ft. All distances fall within the competition-specified recovery distance of 2,500 ft. Blank sections in Figure 11 and Figure 12 indicate temporary loss of [GPS](#) lock.

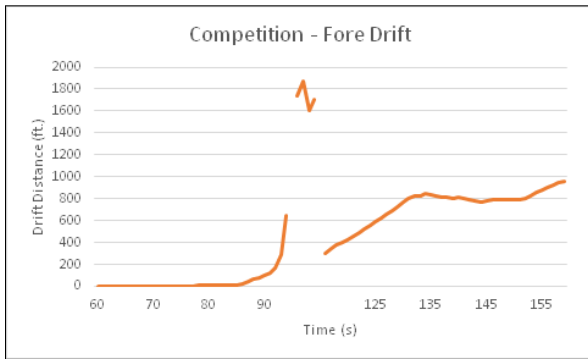


Figure 11: Fore section drift

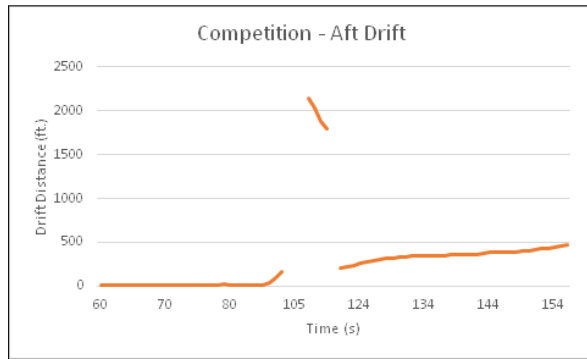


Figure 12: Aft section drift

### 3.4.3 Coefficient of Drag

The drag coefficient was estimated based on altimeter data to be 0.456 for the flight on April 6th, 2019. Moving average filtering was used to reduce noise in the altimeter data, then all four altimeters were averaged to determine an estimated drag coefficient. The reference area was chosen to match reference area in OpenRocket simulations so the values could be directly compared. The reference area is the cross sectional area of the 6.25 in. diameter airframe, or  $30.7 \text{ in}^2$ . A subset of the data was analyzed to determine the drag coefficient. Only data from 5 seconds after takeoff was considered, due to the motor burn. Additionally, data after 10 seconds was not considered due to flight angle of the launch vehicle becoming significant. As flight angle from vertical trajectory increases, horizontal velocity increases. The altimeter data only correlates pressure difference with altitude. Therefore, horizontal velocity is not measured or able to be taken into consideration for this drag coefficient estimation. In summary, only data from 5 seconds to 10 seconds was considered for all 4 altimeters to determine the drag coefficient. Shown in Figure 13 is a plot of the drag coefficient throughout flight based on altimeter data.

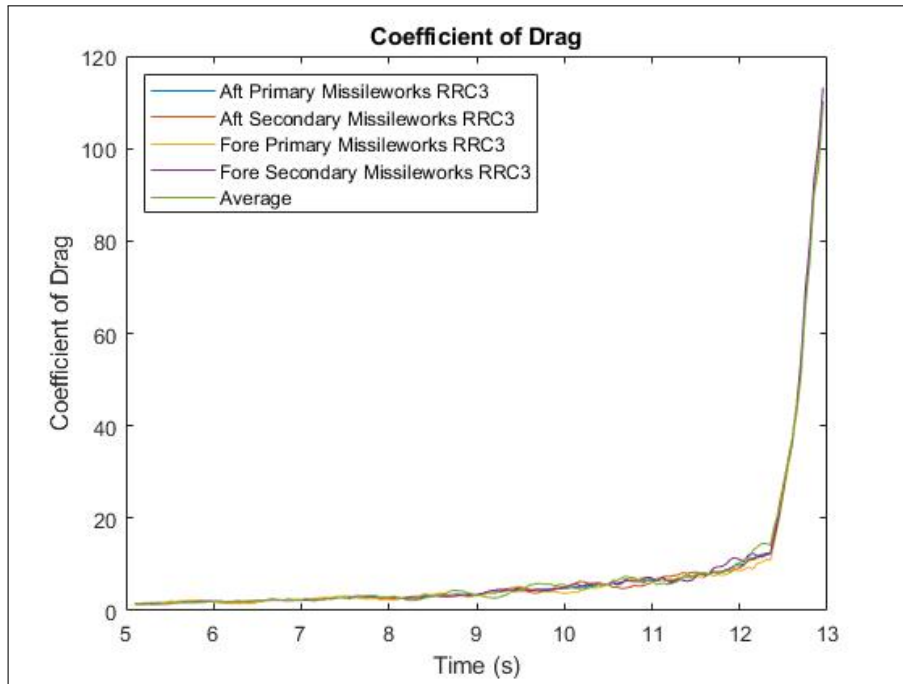


Figure 13: Drag coefficient based on altimeter data

The same process was taken to determine the drag coefficient for OSRTs February 22nd, 2019 and March 16th, 2019 flights. These flights yielded drag coefficients of 0.471 and 0.448 respectively. All drag coefficients agree well with each other based on experimental data. The drag coefficient produced by OpenRocket simulations is 0.399, slightly lower than the experimental data collected. The difference between simulations and actual data can largely be attributed to uncertainty in measurements, especially because only vertical velocity is measured using the altimeter data.

### 3.5 Flight Anomalies

Two anomalies occurred at the competition launch on April 6th, 2019. The major anomaly was the recovery system in the aft section of the launch vehicle. The main parachute in the aft section of the launch vehicle failed to deploy causing the vehicle to land under drogue only, with significantly higher kinetic energy than intended. The camera system also had battery failure prior to launch, causing footage from the launch to not be captured. The camera system was not launch critical, so it was not able to be armed and disarmed from the exterior of the airframe.

### 3.5.1 Recovery Anomaly

During the recovery, the fore airframe section recovered exactly as intended. This provided for a safe delivery of the payload. The aft section, however, became tangled upon ejection. This prevented the main parachute from being deployed, resulting in a landing kinetic energy well above 75 ft-lbf. Altimeter data from the launch indicates that all charges and retention devices performed as intended. Post flight inspection of the ejection charges and Tender Descenders confirmed that all charges ignited, and all Tender Descenders released. Figure 14 shows that the deployment bag was outside of the airframe during recovery, which means all redundancies performed properly to ensure the deployment bag exited the airframe. Despite the deployment bag exiting the airframe, the parachute was unable to escape the bag. Figure 14 proves the ejection charges and retention devices performed correctly.



Figure 14: Aft airframe during recovery

The reason for the failure was determined through post-launch inspection of the recovery subsystem. Figure 15 shows the best picture of the tangled recovery system. It appears that the shroud lines of the parachute wrapped around the connection point of the deployment bag and the shock cord. The layout of the shock

cord allows for the deployment bag section of the shock cord to be pulled away from the knot on the shock cord that connects the main parachute. This ensures the parachute will be pulled out of the deployment bag. This tangled shroud line essentially kept these two shock cord sections close together, preventing the parachute from being pulled out.



Figure 15: Tangled shroud lines

Using a single recovery compartment for both the drogue parachute and the main parachute runs the risk of entanglement upon ejection. Both recovery subsystems were packed correctly in the fore and aft airframe, verified by an inspector and assembler according to the checklists. The packing method was the same method used in the previous successful launches. This occurrence of entanglement is best mitigated by using a two compartment recovery design. In the future, OSRT would like to incorporate a two compartment recovery system if possible to reduce the risk of entanglement.

### 3.5.2 Camera System Anomaly

The batteries in the camera system died before launch. This system is not able to be armed from the launch rail due to design constraints which were not initially considered to be a problem in regards to battery life. Because the system was not launch critical, OSRT did not want to arm the system from the exterior of the airframe, which would have necessitated more holes in the airframe. The OSRT interpreted the launch day schedule to require the launch vehicle to be prepared for the second volley by 10:00 am. However, the arming procedures were significantly delayed from what OSRT anticipated, not beginning until after 11:15 am. The last captured footage from the 360° camera system was during igniter insertion by the Range Safety Officer (RSO). This failure did not occur during previous launch attempts because OSRT did not

have to wait for other launch vehicles to be prepared for launch. To prevent this failure in the future, the cameras should be armed from the exterior of the vehicle. The failure of the camera system did not impact the performance of the launch.

### 3.5.3 *Damage Summary*

The fore section of the launch vehicle did not experience any visible damage due to the successful deployment of the recovery system in that section. The aft section did see minor damage to the canister, BEAVS, airframe and ejection bay. As shown in Figure 16, there is a visible cracks on one side of the canister. The OSRT has concluded the damage was caused by the high kinetic energy landing of the aft section of the launch vehicle. Figure 14 displays the orientation the aft section of the launch vehicle was falling under drogue, which had the coupler hitting the ground first. Therefore, it is unsurprising that the coupler failed upon landing.



Figure 16: Canister Damage

The hard impact also caused the BEAVS motor mount to break, dislodging the motor which can be seen in Figure 17. The motor, once loose, impacted the inner side of the airframe. The cracked airframe is shown in Figure 18. This damage did not occur on either previous full scale flight, because the launch vehicle successfully deployed main parachutes on both flights.

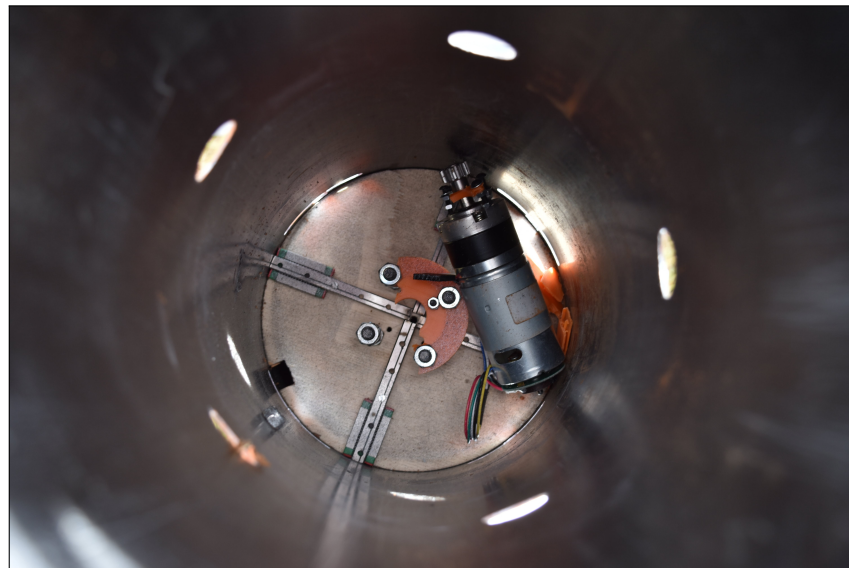


Figure 17: BEAVS Damage



Figure 18: Airframe Damage

Figure 19 depicts the aft ejection bay damage. There were small cracks, throughout the additively manufactured **Polylactic Acid (PLA)** avionics mount however there was no actual damage to the avionics board itself.

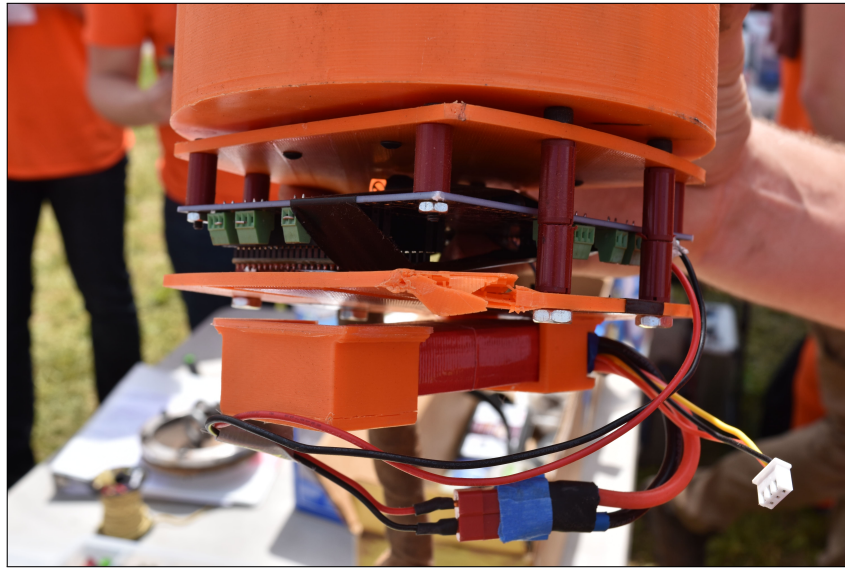


Figure 19: Aft Ejection Bay Damage

Although several components in the aft section of the launch vehicle would need repairs or modifications, **OSRT** feels the vehicle could be reflown. Prior to a reflight of the vehicle, compression testing of the airframe to 15 G's to ensure the airframe would not buckle on ascent would need to be performed with a compression test according to the team derived requirement LV-9, as described in the **OSRT Flight Readiness Review (FRR)** report. The equipment at the **Oregon State University (OSU) Machine Product and Realization Laboratory (MPRL)** does not allow for the full aft section of the airframe to be placed in the Instron compression test machine. Therefore, full certification of the airframe for reflight has not been performed. Additional certification of the airframe could be performed through ultrasonic testing of the airframe, which is available at the **OSU MPRL**, however **OSRT** is not trained on the use of that equipment. Because the airframe does not need to be reflown, **OSRT** did not receive the training to use the ultrasonic testing equipment.

### 3.6 Differences Between Predicted and Actual Data

The drift data recovered from both **ATUs** is reasonably approximate to the data gathered from simulations written and run by the **OSRT** prior to **FRR**. The fore section final drift radius of 633 ft fell within both of the estimated drift distances from OpenRocket and the **OSRT** MATLAB script under 5 to 10 mph wind speeds (492 - 984 ft and 369 - 711 ft, respectively). The aft section final drift radius of 897 ft fell within the

values estimated by the MATLAB script between 5 and 10 mph wind speeds (from 519 to 1,039 ft), but fell above the same range generated by the OpenRocket simulation (369 to 711 ft), though stayed within the 10 to 15 mph wind speed range for the OpenRocket simulation (711 to 1,071 ft). These simulations were performed assuming constant wind speed, which in reality varies over time and with altitude. Therefore, the differences in the drift simulations from the actual data fall within the expected range.

The predicted descent time of the fore and aft sections were 67.07 and 70.83 seconds. The fore section descended in 65.4 seconds, which is slightly faster than simulated. The difference is likely due to the main parachute opening slightly later than simulated. The aft descended in 54.1 seconds. Assuming the aft main parachute had inflated at the same altitude the fore main parachute inflated and assuming the aft fell at the predicted descent rate under drogue and main, it would have landed 84.60 seconds from apogee.

The predicted landing kinetic energy for the fore section was 64.1 ft-lbf. The fore section landed at 65.4 ft-lbf. Since the aft section landed under only a drogue parachute, the predicted landing kinetic energy was 3922.4 ft-lbf. The aft section actually landed with a kinetic energy of 1404.9 ft-lbf. The aft section velocity fluctuated between 50 ft/s and 120 ft/s, falling with an average velocity of 85 ft/s. The aft section was in one of the dips of the fluctuations, impacting at 65.21 ft/s. This resulted in a lower than predicted impact kinetic energy. The predicted impact kinetic energy for the nosecone was 17.9 ft-lbf, and it landed at 15.71 ft-lbf.

With the ballast bay set to 0.5 lbf in the aft section of the launch vehicle and a 5° angle on the launch rail, the simulated apogee was 4,507 ft. The scoring altimeter at competition audibly output 4,548 ft. Analysis of the raw data from the altimeters shows an actual apogee altitude of 4,505 ft. The actual altitude is very close to the predicted altitude performance, within noise ranges of the altimeter, and variations in wind speed during flight.

## 4 PAYLOAD SUMMARY

### 4.1 Payload Overview

The payload objective is to travel at least 10 ft from the launch vehicle after landing, collect a 10 mL soil sample, and store the sample in an on-board containment unit. During competition, the fore section of the airframe successfully landed under the main parachute. The [PEARS](#) retained the payload during flight and ejected the payload using the [Payload Ejection Controller \(PLEC\)](#). However, due to the field conditions and an unfortunate ejection location, the rover landed high-centered on a tilled mound with both wheels unable to contact the ground. The rover failure to drive prevented the rover from proceeding to the soil collection phase of the mission, resulting in the [Soil Collection and Retention \(SCAR\)](#) never attempting to collect a soil sample. This resulted in the payload failing to collect and seal a soil sample.

### 4.2 Data Analysis and Results

The rover was successfully retained during flight operations and ejected upon landing. However, the rover landed atop a recently tilled mound with both wheels in the air, unable to contact the ground and removing the ability to drive. The electrical system triggered the self-righting maneuver and then attempted to autonomously drive. The sonar sensors detected the obstacle in front of the rover and attempted to turn by rotating its right wheel. Because the rover was unable to move, it failed to reach the team specified distance of 50 ft from the airframe which was required to proceed with the soil collection phase of the mission. The team chose a distance of 50 ft from the airframe based on testing to ensure the rover was more than 10 ft from any part of the launch vehicle before attempting to collect soil, taking noise from the [GPS](#) data received into account. Testing performed for the [FRR](#) according to Payload-1 determined the soil collection and retention system was capable of collecting soil.

### 4.3 Payload Anomalies

The payload ejection was completed in a field with conditions worse than those for which the payload was designed. At the start of the project, [OSRT](#) reviewed footage from the 2017-2018 competition and members who attended the competition outlined a set of requirements the payload must meet. The primary requirement was to be able to drive over large clumps of soil. This requirement was met in design through maximizing wheel diameter to increase ground clearance and ensuring enough motor torque to climb a 30° slope. However, upon arrival at the launch site, the team discovered field conditions were significantly worse than designed for. The soil had recently been tilled, and ridges approximately 8-10 in. high were spread consistently throughout the field. Figure 20 displays the field conditions which [OSRT](#) designed

for, based on footage from the 2017-2018 competition, while Figure 21 displays the conditions which were present at the launch site.



Figure 20: 2017-2018 Field Conditions



Figure 21: 2018-2019 Field Conditions

Upon payload ejection, the rover landed high-centered, directly atop the middle of a ridge, as shown in Figure 22. Neither wheel was able to contact the ground enough to drive the rover forward. This caused the rover to not reach the minimum required distance according to the [GPS](#) to begin the soil collection routine. Therefore, after payload ejection, the rover failed to navigate the minimum distance from the airframe and

collect soil. The [OSRT](#) attributes this to a system requirements failure at the start of the project; the payload was never designed to traverse the conditions present at the launch site.



Figure 22: Rover Landing Spot

#### 4.4 Visual Observations

Upon landing high centered in the field, the left wheel of the payload was spinning while the right wheel was stationary. This represents the condition where the right sonar detects an obstacle and attempts to navigate away. Due to the wheels not having proper ground contact, the rover was never able to move past this point before being turned off.

The distance of the payload from the fore section of the airframe was measured to be 17 ft 0 in., while the distance from the nosecone was measured to be 9 ft 5 in., and the distance from a part of the shock cord was measured to be 4 ft 4 in. These distances were all achieved exclusively by the payload ejection; no driving was able to take place. Figures [23 - 28](#) depict the measurements taken of the payload ejection distances.



Figure 23: Distance from the fore airframe



Figure 24: Fore measurement



Figure 25: Distance from the nosecone



Figure 26: Nosecone measurement



Figure 27: Distance from the shock cord

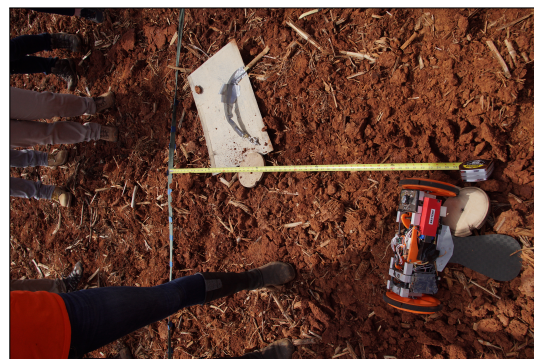


Figure 28: Shock cord measurement

#### 4.5 Scientific Value

One of the focuses of [OSRT](#) throughout the year was the scientific value the payload added to the mission. The [OSRT](#) recognized the significance of collecting a soil sample in simulating a scientific mission on an

extraterrestrial planet, such as Mars. However, collecting the soil sample only represents one phase of the scientific mission. To complete a scientific mission, data from the soil sample needs to be analyzed. To do this, [OSRT](#) designed and built a scientific base station for the rover to dock with and deposit the soil sample. The purpose of the scientific base station was to allow [OSRT](#) to complete a modular experiment design, where any scientific analysis on the soil desired could be completed. The scientific experiment selected was a pH experiment, where soil was deposited into a solution of deionized water through a grate. A pH sensor was actuated into the beaker containing a mixture of soil and deionized water. The pH was then measured until the sensor reached a steady state value after 90 seconds and broadcast raw data and [GPS](#) coordinates of the soil collection region back to the ground station via an Xbee over 900 MHz transmission. The rover was then to leave the scientific base station, collect an additional soil sample, and return to the base station. Shown in Figure 29 is the scientific base station which was constructed for the mission.

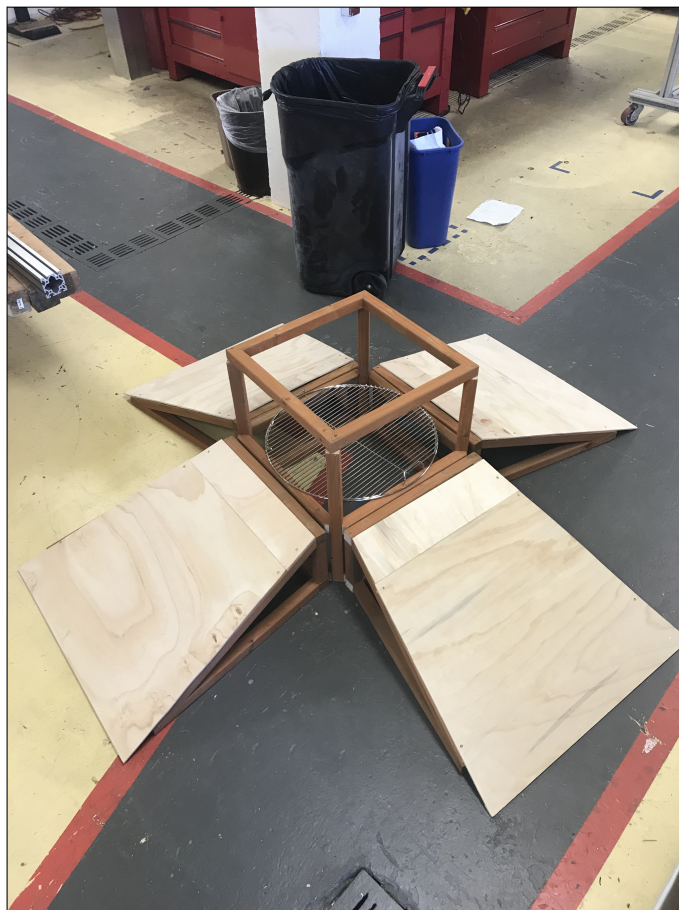


Figure 29: Scientific Base Station

Ultimately, the [National Aeronautics and Space Administration \(NASA\)](#) stated mission was prioritized

over the scientific base station. Therefore, the rover was never successfully able to complete the docking procedure with the scientific base station.

The payload landed in a position which prevented all motion, deeming the rover mission a failure. Despite the payload mission failure, **OSRT** feels there is significant scientific value added in attempting the mission which **OSRT** chose. The **OSRT** feels the landing position of the rover was unfortunate, and the conditions of the field exceeded the design requirements of the payload. However, the mission which was attempted, to collect and seal a soil sample, deliver it to a scientific base station, and analyze the pH of the soil sample adds significant scientific value to the project. The **OSRT** mission design represents a small scale version of an actual extraterrestrial mission. The team had to perform: a launch, recovery, safe landing, rover deployment, rover navigation, soil collection, soil retention, soil deposition, and soil analysis. While the team only successfully completed the stages up to rover deployment, the other elements were completed in design and required significant planning throughout the entire duration of the project. Successful performance of all elements of the **OSRT** mission on an extraterrestrial planet could be used to inform future missions on locations for follow up missions which require soil with a specific pH balance. An example of a mission which could require this would be a future mission to plant and harvest crops to sustain human life on an extraterrestrial planet.

## 5 PROJECT PLAN

### 5.1 Budget Summary

The [OSRT](#) was fortunate to be supported in part by the [NASA Oregon Space Grant Consortium \(OSGC\)](#) grant NNX15AJ14H. In addition to [OSGC](#) support, [OSRT](#) received support from the [OSU](#) chapter of [American Institute of Aeronautics and Astronautics \(AIAA\)](#) and several corporate sponsors. Some of these sponsors include [ICE](#), [Allegheny Technologies Incorporated \(ATI\)](#), Eugene Home Comfort, and Woodstocks Pizza. The project would not be possible without the continued support of [OSRT](#) by these organizations.

Table 7: Major funding contributions breakdown.

	Total Cost	OSGC Contribution	Matching Contribution	Matching Sources
Structures	\$6,151.98	\$3,042.00	\$3,109.98	<a href="#">ICE</a> , Fiberglass, Club Resources
Aerodynamics and Recovery	\$2,987.84	\$2,824.26	\$163.58	Club Resources
Payload	\$2,977.28	\$2,172.44	\$804.84	Club Resources
Outreach	\$300.00	-	\$300.00	<a href="#">AIAA</a>
Travel	\$10,760.58	-	\$10,760.58	<a href="#">AIAA</a> , Student Expenditure
Lodging	\$5,100	\$2,961.30	\$2,138.70	<a href="#">AIAA</a> , Student Expenditure
Total	\$28,277.68	\$11,000.00	\$17,277.68	
		Matching Ratio: 1.57		

### 5.2 STEM Engagement Summary

Over the course of the [NASA SL](#) project timeline, [OSRT](#) engaged with 3,362 members of our community with [Science, Technology, Engineering and Mathematics \(STEM\)](#) related topics and activities. Our [STEM](#) engagement ranged from classroom presentations about our project, launching straw rockets with a compressed air launcher, chemistry and physics experiments, and general engineering discussions with students ranging as young as pre-school to as old as college. We also engaged in adults throughout the project, in hopes they will help us inspire the next generation to pursue [STEM](#) related careers.

[OSRT](#) has continued [STEM](#) engagement in our community outside of the project timeline. Three events have occurred since the [STEM](#) Engagement deadline, and more are scheduled this spring and summer. A comprehensive list of all contacts for [STEM](#) engagement was created and will be passed to next year's [OSRT SL](#) team along with lesson plans used by the 2018-2019 team and more that were not able to be used. There

are many contacts around the Pacific Northwest that this years team was not able to visit. Next year's [OSRT](#) is setup to engage more members of our community with improved lesson plans and encourage [STEM](#) education for the next generation.

## 6 LESSONS LEARNED

The most important lesson learned was from the payload mission failure. This lesson is to accurately define all system requirements prior to the design phase. Because [OSRT](#) misidentified of the worst case scenario for the landing site that the rover would have to drive, the rover became stuck and unable to move itself. The lack of movement prevented the rover from proceeding to the soil collection phase and resulted in mission failure.

An additional lesson learned was scope creep. The [OSRT](#) hoped to perform an additional scientific mission with the soil sample that was collected, however on an already short project timeline, the rover docking with the scientific base station was never able to be completed. The [OSRT](#) plans to continue to improve on the rover and implement functionality allowing the rover to dock with the scientific base station beyond the extent of the competition timeline. Despite not being successfully implemented into the final payload mission at the competition, [OSRT](#) feels this was a valuable part of the experience, challenging students to solve problems that made the mission more closely simulate an extraterrestrial mission.

## 7 EXPERIENCE SUMMARY

The [OSRT](#) learned many important lessons and developed skills to become more successful engineers in the future. This is only the second year [OSRT](#) has been a part of [Student Launch Initiative \(SLI\)](#), which means the team is still developing tools for success. The project management tools saw great improvement throughout the year, particularly aiding in better performance in documentation as the year progressed. The team was able to cohesively work together and build skills for problem solving technical challenges. In addition to technical work, nearly every member of the team dealt with conflict resolution at some point during the project, each member developing methods to resolve the type of conflicts which arise in work environments and team projects.

Many of the members of [OSRT](#) completed the project as a part of a senior design capstone course. The project required significantly more time and dedication to complete successfully than the typical senior design capstone courses at [OSU](#), however the majority of the students who completed the project feel that it was a very rewarding experience which helped to prepare them for careers in the [STEM](#) field.